catalysts

MDPI

Article

Impact of TiO_2 Surface Defects on the Mechanism of Acetaldehyde Decomposition under Irradiation of a Fluorescent Lamp

Piotr Rychtowski [1], Beata Tryba [1,*], Hubert Fuks [2], Maria Ángeles Lillo-Ródenas [3] and Maria Carmen Román-Martínez [3]

[1] Department of Catalytic and Sorbent Materials Engineering, Faculty of Chemical Technology and Engineering, West Pomeranian University of Technology in Szczecin, Piastów Ave. 42, 71-065 Szczecin, Poland; rp43903@zut.edu.pl

[2] Faculty of Technical Physics, West Pomeranian University of Technology in Szczecin, Piastów Ave. 17, 70-310 Szczecin, Poland; hubert.fuks@zut.edu.pl

[3] Department of Inorganic Chemistry and Materials Institute, Faculty of Sciences, University of Alicante, Carretera de San Vicente del Raspeig s/n, 03690 Alicante, Spain; mlillo@ua.es (M.Á.L.-R.); mcroman@ua.es (M.C.R.-M.)

* Correspondence: beata.tryba@zut.edu.pl

Abstract: TiO_2 was placed in heat-treatment at the temperature of 400–500 °C under flow of hydrogen gas in order to introduce some titania surface defects. It was observed that hole centers in TiO_2 were created during its heat treatment up to 450 °C, whereas at 500 °C some Ti^{3+} electron surface defects appeared. The type of titania surface defects had a great impact on the mechanism of acetaldehyde decomposition under irradiation of artificial visible light. Formation of $O^{\bullet -}$ defects improved both acetaldehyde decomposition and mineralization due to the increased oxidation of adsorbed acetaldehyde molecules by holes. Contrary to that, the presence of electron traps and oxygen vacancies in titania (Ti^{3+} centers) was detrimental for its photocatalytic properties towards acetaldehyde decomposition. It was proved that transformation of acetaldehyde on the TiO_2 with Ti^{3+} defects proceeded through formation of butene complexes, similar as on rutile-type TiO_2. Formed acetic acid, upon further oxidation of butene complexes, was strongly bound with the titania surface and showed high stability under photocatalytic process. Therefore, titania sample heat-treated with H_2 at 500 °C showed much lower photocatalytic activity than that prepared at 450 °C. This study indicated the great impact of titania surface defects (hole traps) in the oxidation of acetaldehyde and opposed one in the case of defects in the form of Ti^{3+} and oxygen vacancies. Oxidation abilities of TiO_2 seem to be important in the photocatalytic decomposition of volatile organic compounds (VOCs) such as acetaldehyde.

Keywords: TiO_2; oxygen surface defects; FTIR; thermal desorption; acetaldehyde decomposition

Citation: Rychtowski, P.; Tryba, B.; Fuks, H.; Lillo-Ródenas, M.Á.; Román-Martínez, M.C. Impact of TiO_2 Surface Defects on the Mechanism of Acetaldehyde Decomposition under Irradiation of a Fluorescent Lamp. *Catalysts* **2021**, *11*, 1281. https://doi.org/10.3390/catal11111281

Academic Editor: Juan Matos Lale

Received: 3 October 2021
Accepted: 21 October 2021
Published: 23 October 2021

1. Introduction

The photocatalytic purification of air from volatile organic compounds (VOCs) has been an interesting subject of study for many research groups [1–3]. One of the targets is improvement of the quality of indoor air by reducing the amount of VOCs, which can be responsible for symptoms called "sick building syndrome" [4].

The most explored material which is used in indoor air purification is TiO_2. The research group of Prof. A. Fujishima published many papers related to the photocatalytic properties of TiO_2 towards environmental cleanup [5–7]. They proposed the mechanism of acetaldehyde decomposition, which involved radical-initiated chain reactions with oxygen consumption [5]. They noticed that adsorbed molecules could react with photogenerated holes and contribute in the suppressing of recombination of free charges. They reported

that formed holes (h^+) mediated in the reaction of carbonyl radicals formation, according to the reaction [8]:

$$3\ CH_3CHO + O_2 + h^+ \rightarrow 2\ CH_3COOH + CH_3CO^\bullet + H^+$$

Carbonyl radicals ($CH_3CO^\bullet$) take part in the reactions of acetaldehyde oxidation [8]. Acetic acid is the main intermediate product during acetaldehyde oxidation. Hole scavenging by organic adsorbates on the TiO_2 surface was also discussed by other researchers [9]. Formation of carbonyl radicals and their share in photooxidation reactions can increase the yield of the photocatalytic process. Therefore, adsorption of acetaldehyde on the titania surface seems to be a crucial step in photocatalytic reactions. Adsorption of acetaldehyde on TiO_2 depends on its specific surface area, hydroxylation state, and dominant crystal face [10–12]. Anatase-type TiO_2 of high surface area and low quantity of hydroxyl groups usually exhibits high adsorption and photocatalytic activity towards acetaldehyde decomposition. Moreover, the titania sample with a dominant anatase face (001) showed higher adsorption and photocatalytic conversion of acetaldehyde than these, which had dominant faces of anatase (101) and (010) [12]. It was also reported that acetaldehyde was adsorbed to a higher extent on the reduced anatase and rutile than on their oxidized forms [13,14]. The mechanism of acetaldehyde adsorption and its further transformation on TiO_2 differs between its reduced and oxidized structure. It has been found that acetaldehyde molecules undergo adsorption preferentially via oxygen vacancies sites in the reduced titania, followed by formation of butene complex. Contrarily, on the oxidized TiO_2, acetaldehyde forms oxygen complexes and then is oxidized to acetate [13,14]. Many experimental studies have shown that adsorbed acetaldehyde on the titania surface was followed by an aldol condensation to form 3-hydroxybutanal and crotonaldehyde, but partly was oxidized to acetate [15,16]. Crotonaldehyde can be photocatalytically converted to acetate and formate species. The formed formate species can be further oxidized to formic acid and CO_2 [15,16]. Physically adsorbed acetaldehyde on the titania surface is undergoing reversible desorption, whereas that which is chemisorbed follows further transformation [10,11]. Therefore, high adsorption of acetaldehyde on the titania surface does not guarantee its high photocatalytic conversion [10]. Recently, the group of Prof. A. Fujishima reported that TiO_2 modified through a solution plasma process exhibited high photocatalytic activity towards acetaldehyde decomposition [8]. The solution plasma process caused transformation of anatase to brookite and formation of some surface defects. Most likely, these structural changes were responsible for enhanced activity of TiO_2. Such modification caused formation of oxygen vacancies and adsorption of hydroxyl groups from the atmosphere (confirmed by XPS measurements). The authors explained that, when oxygen vacancies were created on the TiO_2 surface, oxygen adatoms attached to these sites and formed hydroxyl groups through $O_2^{\bullet -}$ radicals [8]. They also mentioned that the optical structure of such solution plasma-modified TiO_2 is quite different than that formed through nitrogen modification. In their experiments, the oxygen vacancies were located below the conduction band as surface state and did not show any shift of the optical band edge but instead featured enhanced absorbance in the tail part of the visible-light region [8]. Moreover, they reported that both ESR and XPS analyses showed that the solution plasma-treated TiO_2 contained no Ti^{3+} centers. In our previous studies, we have proved that the presence of both oxygen vacancies and Ti^{3+} centers formed in TiO_2 upon ammonia modification were detrimental for acetaldehyde decomposition [17]. However, other researchers reported that Ti^{3+} defects, which were formed upon doping of carbon quantum dots to TiO_2, could improve separation of free charges and enhance photocatalytic decomposition of acetaldehyde [18]. However, an observed effect of enhanced photocatalytic activity was caused by the increased yield in formation of superoxide radicals rather than the quantity of Ti^{3+} species [18]. The impact of type and quantity of surface defects in TiO_2 on its photocatalytic properties towards acetaldehyde decomposition is still under scientific debate. From the other side, formation of brookite phase could also improve charge separation in titania material. The composition of anatase and brookite

was found to be beneficial for the photocatalytic oxidation of acetaldehyde, because of possible photoinduced transfer of electrons between anatase and brookite and suppression of recombination reaction for electron/hole pairs [19,20]. The group of Prof. A. Fujishima has also reported that visible-light absorbance of TiO_2 treated by solution plasma process could be influenced by brookite/anatase heterostructure formation [8].

The other problem which is still unsolved relates to the different states of TiO_2, namely, oxidized and reduced. Some researchers observed high reactivity of the reduced anatase with dominant (001) face for the acetaldehyde adsorption [14]. They noticed formation of 2-butanone and butene through the adsorption of paired CH_3CHO molecules at the reduced defect sites via oxygen [14]. However, thermal desorption of 2-butanone and butene caused leaving the oxygen at the titania vacancy sites, so within the time the oxygen vacancies were saturated with oxygen, they could be formed again after annealing of TiO_2 at 850 °C [14]. Formation of butene complexes was also noted on the reduced rutile [13]. On the oxidized rutile, some of the oxygen-acetaldehyde surface complexes were formed. One of these complexes was found to undergo an easy and non-reversible transformation to a highly stable surface acetate, which was desorbed from the surface at high temperature [13]. Although high adsorption of acetaldehyde was noted on the reduced titania in comparison with its oxidized form, there is a lack of information on the impact of such a structure on the yield of photocatalytic oxidation.

The role of titania defects in TiO_2 depends on their quantity and localization. The research studies performed by Di Valentin et al. [21] showed that the presence of Ti^{3+} centers in TiO_2 could form different electronic states in its structure. They differentiated four types of Ti^{3+} centers, 6-fold coordinated, associated with H-doping, undercoordinated, associated with oxygen vacancies and interstitial Ti^{3+} species [21]. Based on DFT calculations, it was proved that various types of Ti^{3+} defects form different localized electron states densities in TiO_2, the interstitial ones are localized at the nearest valence band, but the 6-fold coordinated type are very close to the bottom of the conductive band [21].

Formation of titania defects depends on the preparation method and the modification agent. Higher reduction of TiO_2 can be obtained at higher temperature of heat-treatment [21]. Introducing the reduction agent during TiO_2 preparation can accelerate formation of titania surface defects. The aim of this study was focused on the preparation of TiO_2 with different surface defects and investigation of their role in the photocatalytic decomposition of acetaldehyde. Preparation of TiO_2 under hydrogen treatment was performed. EPR measurements were applied for detection of titania surface defects. The mechanism of acetaldehyde decomposition was elaborated based on FTIR and TPD measurements.

2. Results

The results obtained from XRD and BET measurements are shown in Table 1. In Figure 1, there are the results from XRD measurements.

Table 1. The phase composition, average anatase crystallites size, and BET surface area of the prepared and commercial titania samples.

Sample Name	HTT (°C)	BET Surface Area (m^2/g)	Phase Composition (Anatase: Rutile)	Average Crystallites Size of Anatase (nm)
TiO_2-A-150	150	215	95:5	15.2
TiO_2-400-H_2	400	155	97:3	15.1
TiO_2-450-H_2	450	130	96:4	16.3
TiO_2-500-H_2	500	81	96:4	24.3
TiO_2-400-Ar	400	167	97:3	15.0
TiO_2-450-Ar	450	139	95:5	15.5
TiO_2-500-Ar	500	123	96:4	16.8
TiO_2-600-Ar	600	68	96:4	25.5
Nanorutile	-	122	97:3	5.3
Krono*Clean*®7050	-	322	100:0	6.9

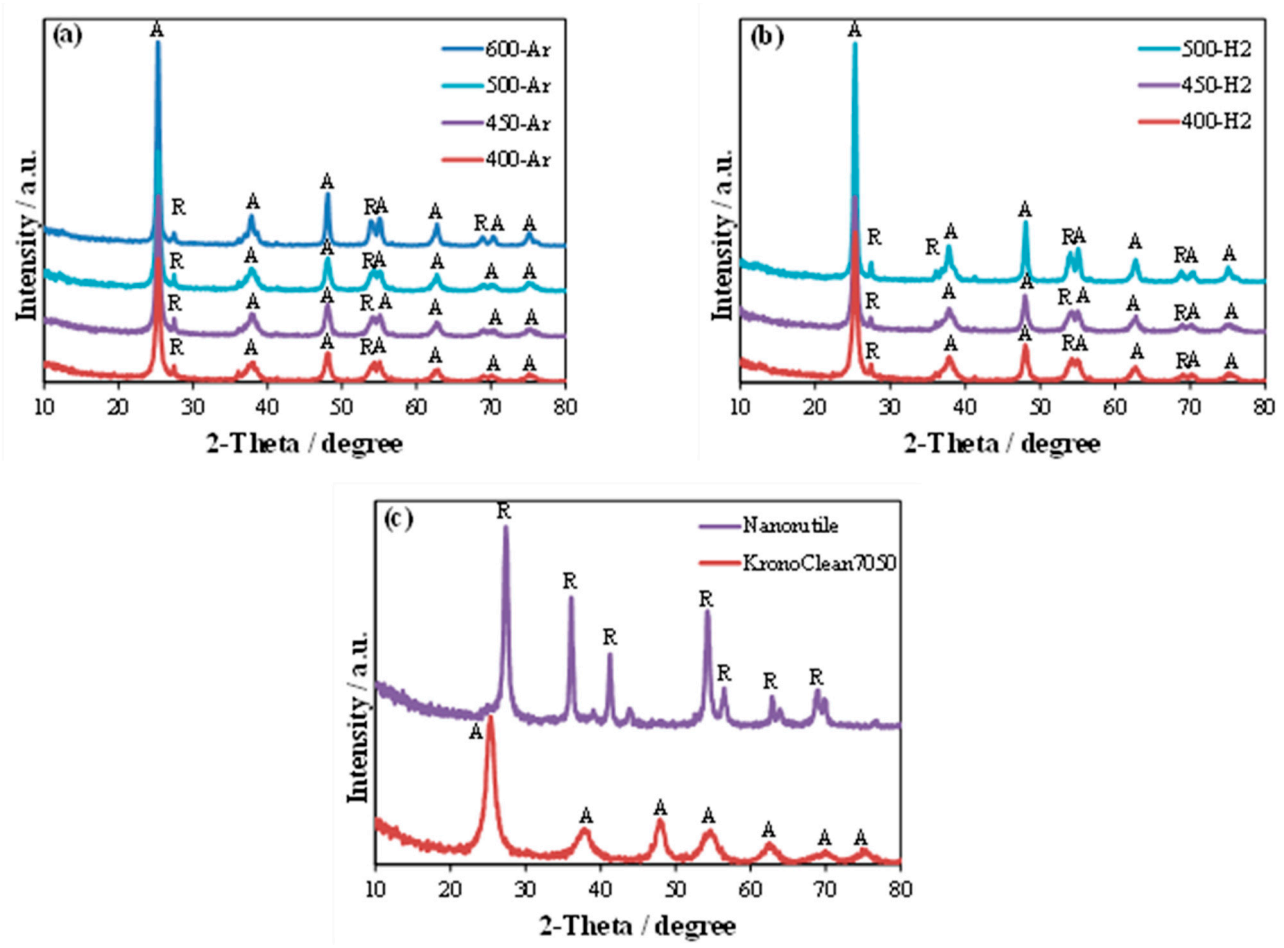

Figure 1. XRD patterns of: (**a**) samples heat treated under argon in 400–600 °C, (**b**) samples heat treated under hydrogen in 400–500 °C, (**c**) commercial samples.

From the comparison of the parameters of titania samples prepared under hydrogen and argon atmospheres, it can be observed that reducing atmosphere of hydrogen accelerated crystallization of anatase. The rapid growth of anatase crystallites took place at 500 °C for titania heated under flow of hydrogen gas, whereas in Ar atmosphere, a similar effect was observed at 600 °C. Hydrogen could be adsorbed on the surface defects of TiO_2 and contributed to the desorption of surface hydroxyl groups. Therefore, amorphous and hydroxylated titania heat-treated under hydrogen could undergo crystallization faster than in argon atmosphere. The phase composition of samples was rather stable.

The optical properties of titania samples were investigated by UV-Vis/DR measurements. The results are presented in Figure S1 (Supplementary Material).

Generally, there was no observed bandgap shift in the absorption edge; only sample heated at 500 °C showed absorption of light in the visible range 400–650 nm. This sample, contrary to others, had brownish color, which probably resulted from the reduction of titania. Hydrogenation of TiO_2 has been widely described in the literature [22–24]. Black TiO_2 can be obtained through various methods, such as the reduction of titania with hydrogen under high pressure and low temperature such as 200 °C [22], reduction under UV and vacuum annealing at 300 °C [23], hydrogenation under atmospheric pressure at temperature of 500 °C and subsequent rapid cooling, hydrogenation plasma treatment, or through reduction with various metals, such as aluminum, zinc, and magnesium [24].

Black color is caused by structural modifications of titania such as: presence of Ti^{3+} through self-doping, surface hydroxyl groups, oxygen vacancies, and Ti-H bonds [24].

The color of sample depends on the reduction method. White TiO_2 can be transformed to gray, blue, brown, or black color, depending on the preparation conditions [22]. The resulting color is ascribed to the formation of various amounts of Ti^{3+} and oxygen vacancies. Increasing the "level" of reduction leads, in general, to a higher density of defects (e.g., Ti^{3+} and oxygen vacancies concentration) and consequently to "darker" TiO_2 powders [22].

In Figure 2, the EPR spectra of titania samples heated under both hydrogen and argon atmospheres were illustrated.

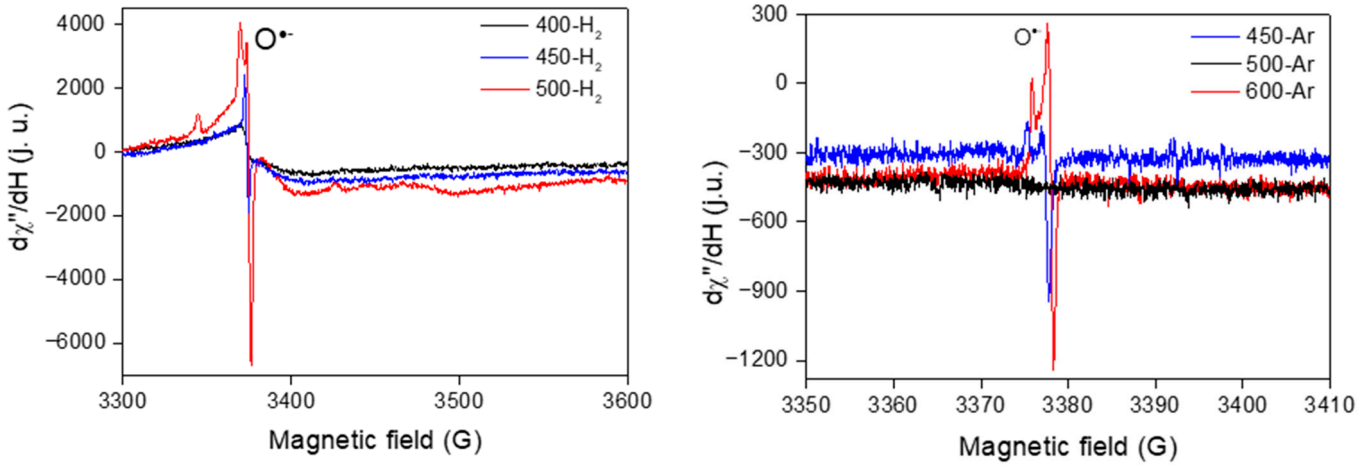

Figure 2. EPR spectra of TiO_2 samples heat-treated at 400–600 °C under hydrogen (**left**) and argon (**right**).

For samples reduced in hydrogen, there was one narrow signal at g = 2.012, which can be assigned to the $Ti^{4+}O^{2-}Ti^{4+}O^{\bullet-}$ on anatase [25]. This signal was the most intensive in sample heated at 500 °C. Additionally, for sample heated at 500 °C some other signals were observed. However, they were very broad and exposed low intensity. Calculated g values for these signals were around 1.988 and 1.971, resulted from the formation of surface Ti^{3+} in solid anatase and rutile phases, respectively [25]. Titania samples heated in argon at 450 and 600 °C showed also one high-intensity signal related to the $O^{\bullet-}$ radicals in anatase. The sample heated in argon at 500 °C did not show any structural defects. It is most likely that at this temperature of heat treatment the whole crystallization of anatase crystals occurred, but at 600 °C self-reduction of anatase took place. The commercial samples, nanorutile and KRONOClean 7050, did not show any signals in the performed EPR spectra.

Formation of hydroxyl radicals on the surface of the titania samples under UV irradiation was measured in an aqueous solution of terephthalic acid. The results related to the formation of the reaction product, 2-hydroxyterephthalic acid, are shown in Figure 3.

In the case of titania samples heated in argon atmosphere, the speed of OH radical formation was accelerated with increasing the temperature of heat treatment during their preparation. This can be related to the increase in their crystallites size and improved separation of free radicals. Impact of anatase crystallites size on the lifetime of free radicals was reported elsewhere [26]. In the case of samples reduced under hydrogen, the highest formation of hydroxyl radicals was noted on sample prepared at 450 °C, although that prepared at 500 °C had higher crystallites size. The commercial samples such as nanorutile and KRONOClean 7050 were also tested for OH radical formation under UV irradiation (Figure 3c). The obtained results showed poor oxidation ability of nanorutile in comparison to KRONOClean 7050, which has an anatase structure. Such low generation of hydroxyl radicals on rutile was caused by its lower oxidation potential in comparison to anatase, and higher reduction abilities [27].

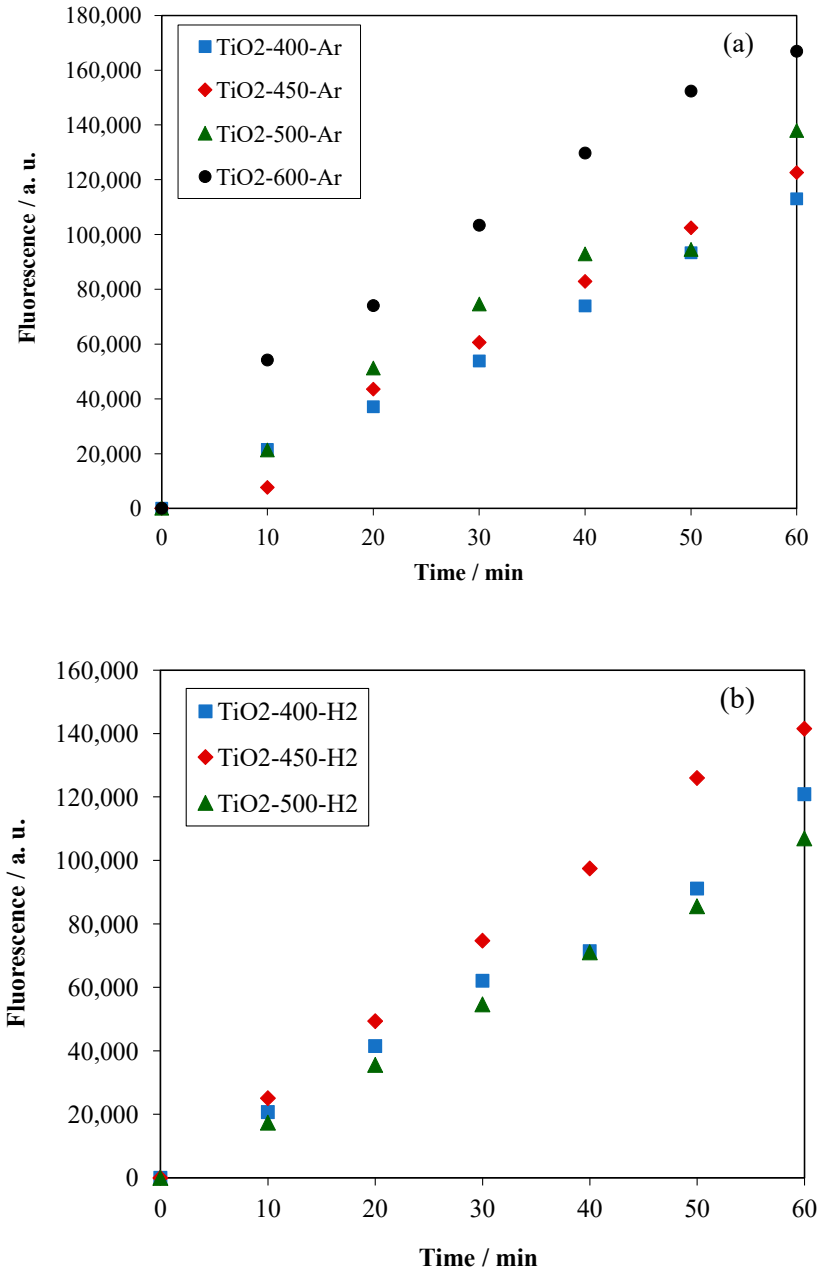

Figure 3. *Cont.*

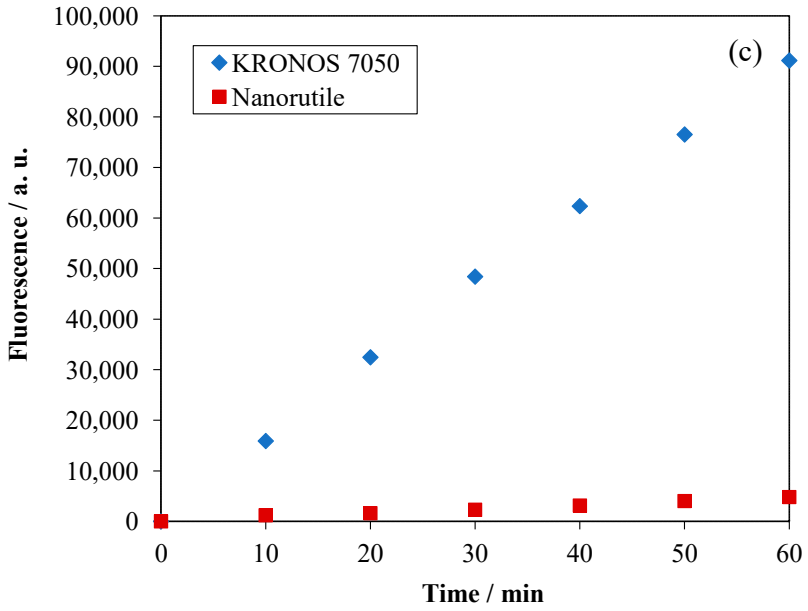

Figure 3. OH radical formation during irradiation of UV light on the prepared titania samples under (**a**) argon, (**b**) hydrogen, and (**c**) commercial.

In the next step, photoluminescence measurements were performed for the prepared and commercial titania samples. The emission spectra were recorded at the wavelength range of 330 to 700 nm after excitation at 290 nm. The results are presented in Figure 4.

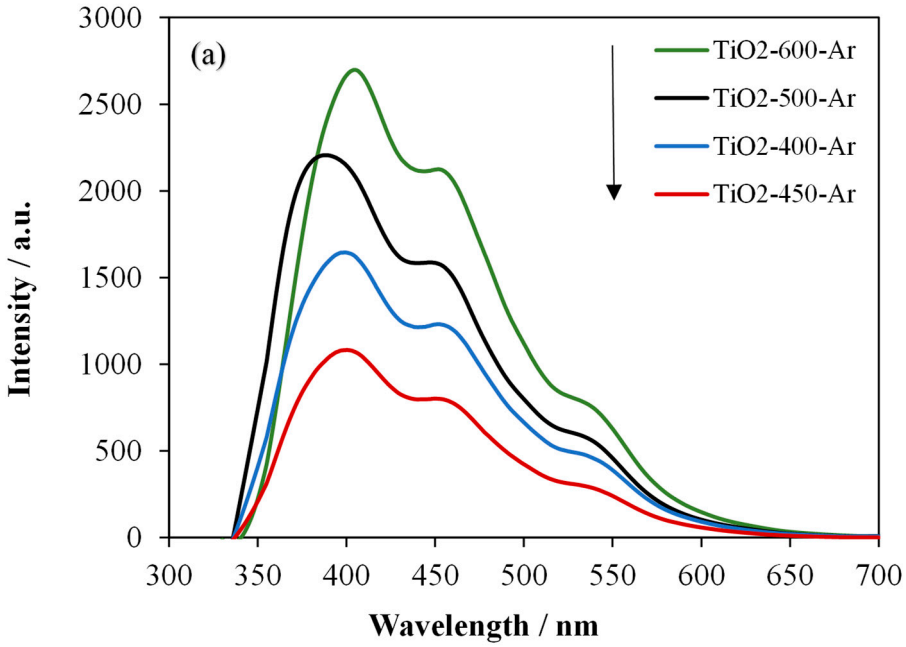

Figure 4. *Cont.*

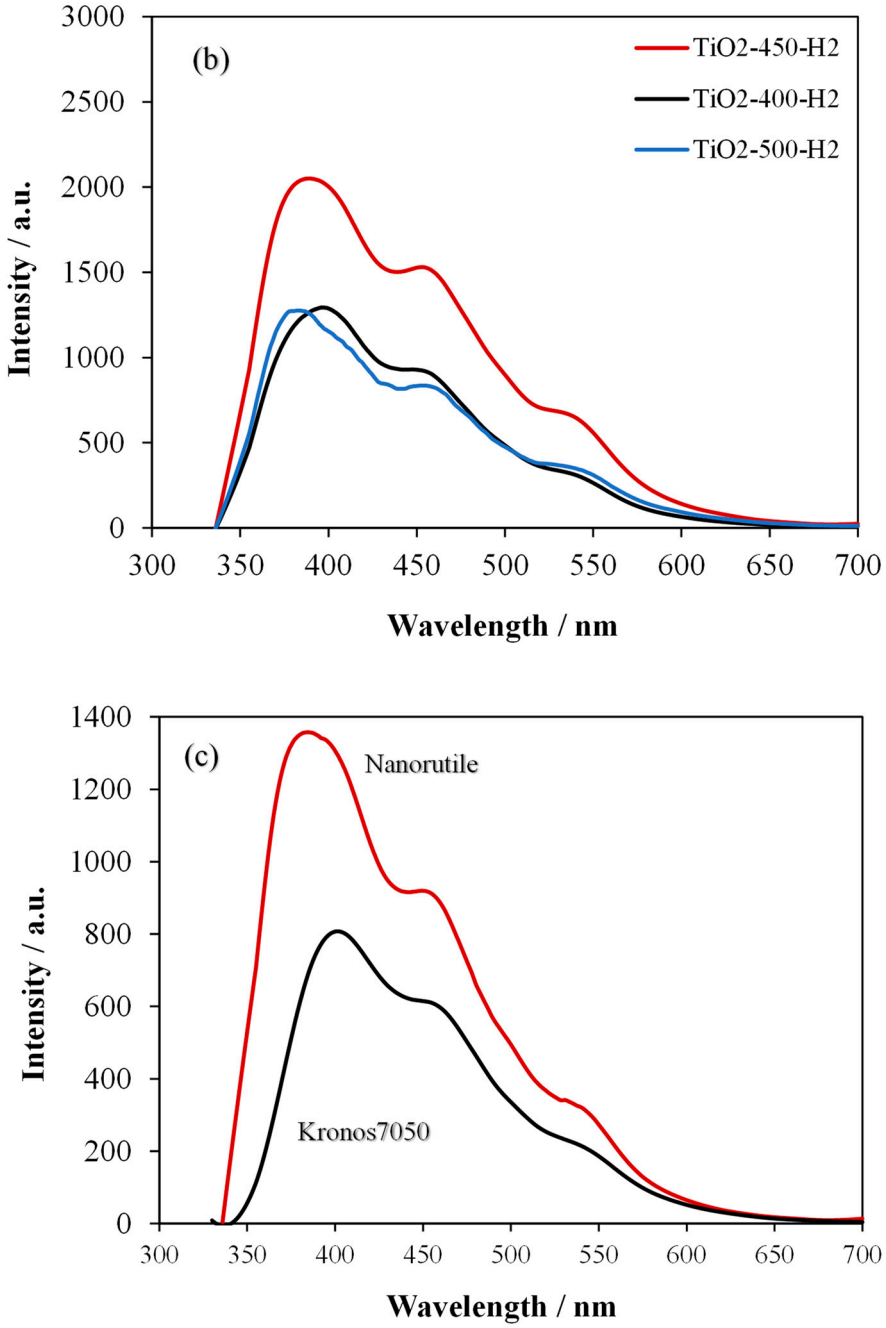

Figure 4. Photoluminescence spectra of titania samples (**a**) heat-treated in argon, (**b**) heat-treated under hydrogen, and (**c**) commercial.

Photoluminescence spectra give information about radiative recombination of free radicals in TiO_2 after its excitation. The recombination process is related to the physico-chemical properties of titania samples, such as: crystallinity and surface defects, phase composition, crystallites size, and the presence of amorphous TiO_2 and some impurities. It was already proved that, during heat-treatment of TiO_2 up to 450 °C, the amorphous part changed to crystalline structure and dehydrogenation of titania surface took place [28]. TiO_2 samples consisting of high-crystallinity anatase such as KRONOClean 7050 and TiO_2-450-Ar showed the photoluminescence emission spectra of low intensity contrary to nanorutile-type TiO_2. Sample prepared at 450 °C under H_2 treatment showed higher photoluminescence intensity than that prepared in Ar atmosphere. The most probably formed surface defects (hole traps) in TiO_2-450-H_2 sample increased recombination of free

carriers. This fact could be explained by an increasing amount of OH groups on the TiO_2 surface through the formed hole-traps defects. During irradiation of TiO_2 at 290 nm, OH radicals were formed by reaction of holes with adsorbed hydroxyl groups. However, they could recombine with electrons in the absence of any organic compound.

Contrary to that, TiO_2-500-H_2 sample showed a lower recombination process. This sample had both kinds of surface defects, hole and electron traps. The presence of electron traps in this titania sample could increase adsorption of atmospheric oxygen on its surface and induce formation of $O_2^{\bullet -}$. This could conduct to suppressing the recombination process.

The prepared samples were tested for the photocatalytic decomposition of gaseous acetaldehyde under irradiation of a fluorescent lamp. The results are presented in Figure 5.

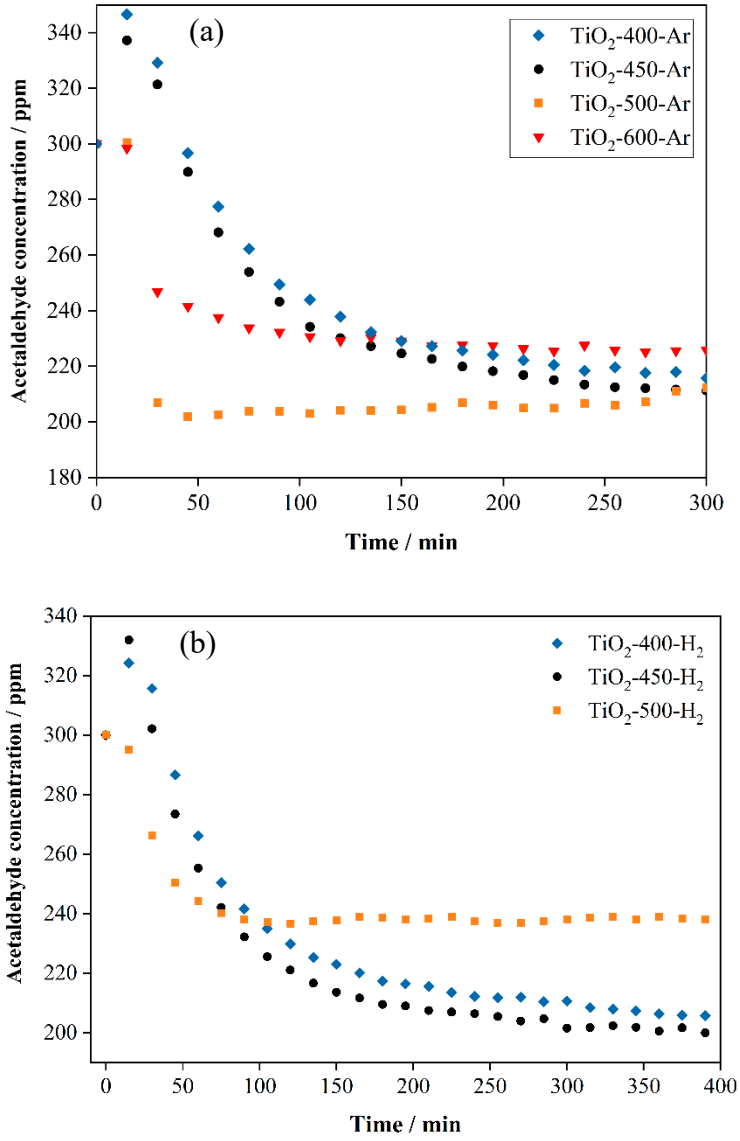

Figure 5. *Cont.*

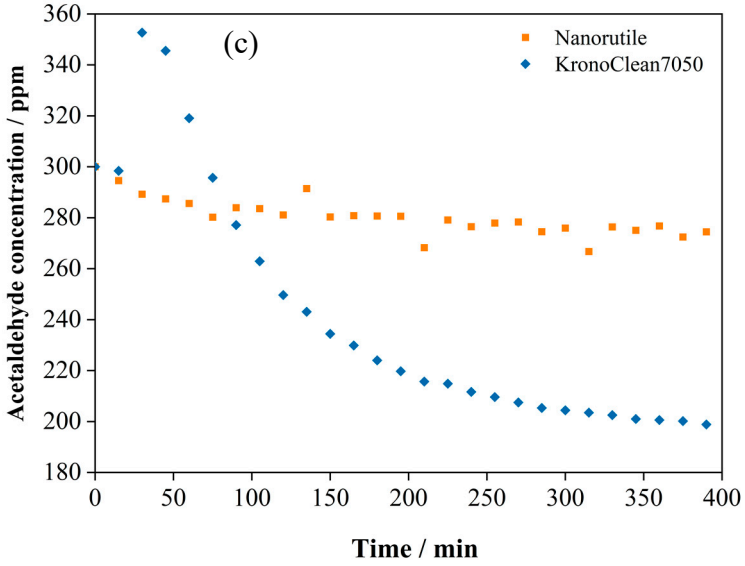

Figure 5. Photocatalytic decomposition of acetaldehyde on the titania samples under irradiation of a fluorescent lamp: heat-treated in Ar (**a**), hydrogen (**b**), and commercial (**c**).

Around 30% of acetaldehyde was decomposed at the flowing rate of gas equal to 20 mL/min. The highest percent of acetaldehyde decomposition was noted on titania prepared at 450 °C under hydrogen. Somewhat lower decomposition was observed on TiO_2 sample prepared at 500 °C in Ar. Generally, samples prepared at higher temperatures showed lower photocatalytic activity. In the case of commercial samples, nanorutile showed poor activity, whereas KRONOClean7050 decomposed acetaldehyde in the quantity of around 30%, similar to the best active sample among all the prepared ones.

Photocatalytic decomposition of acetaldehyde on TiO_2 depends on the interaction of the acetaldehyde molecules with the titania surface and its transformation path upon the photocatalytic process. Therefore, FTIR analysis of the titania surface for selected samples was performed before acetaldehyde adsorption, after adsorption in the dark, and then after the photocatalytic process.

In Figure 6, some FTIR spectra from performed measurements are presented, as original, titania samples do not differ much from each other. However, in the commercial samples were a higher intensity peak at the wavelength of around 3800–2500 cm^{-1}, attributed to the OH group. Additionally, TiO_2 after reduction with H_2 at 500 °C showed a small intensity band at 1518 cm^{-1}. This peak can be assigned to some -COO groups. The, most probably, CO_2 molecules were adsorbed on its surface due to the formed defected structure after hydrogen treatment. Nanorutile also showed some bands at 1435 and 1318 cm^{-1}, which can be assigned to δ CH_3 vibrations [1].

FTIR spectra of the titania samples after acetaldehyde adsorption are presented in Figures 7 and 8. For each sample, both kinds of spectra are presented: originally recorded by spectrometer (Figure 7) and after subtracting the spectrum of pure sample (Figure 8). Titania samples heat-treated in Ar at 500 and 600 °C, and that prepared in H_2 at 450 °C, showed some similarities with bands at the range of 1706–1770 cm^{-1}, which are typical to acetic acid and formate species and can be assigned to ν(C=O) vibrations [15,29,30]. Both samples Ar-500 and Ar-600 indicated the presence of acetate at the wavelengths of 1414 and 1418 cm^{-1} (CH_3 species). However, only Ar-500 samples showed some band of low intensity at 1292 cm^{-1}, assigned to ν(C–O) vibration in the acetic acid. In the case of sample H_2-450 there were observed signals at 1556, 1514, and 1438 cm^{-1}, which indicate the vibration of ν_a(COO) in both acetate and formate species. In the original recorded spectrum of TiO_2-500-H_2 sample, it was difficult to conduct accurate analyses, because observed peaks exhibited very low intensity. However, after subtraction of spectrum recorded for the pure sample, some bands could be clearly observed.

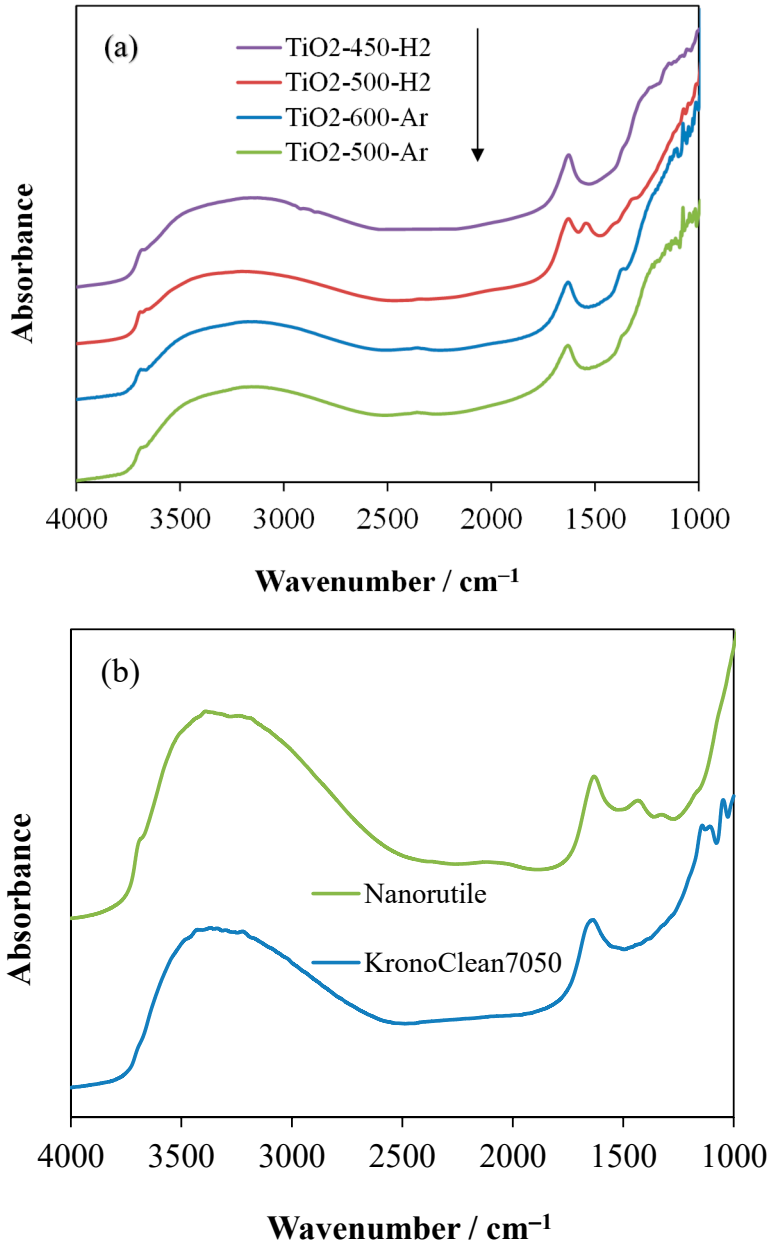

Figure 6. FTIR spectra of the titania samples, (**a**) as prepared and (**b**) commercial.

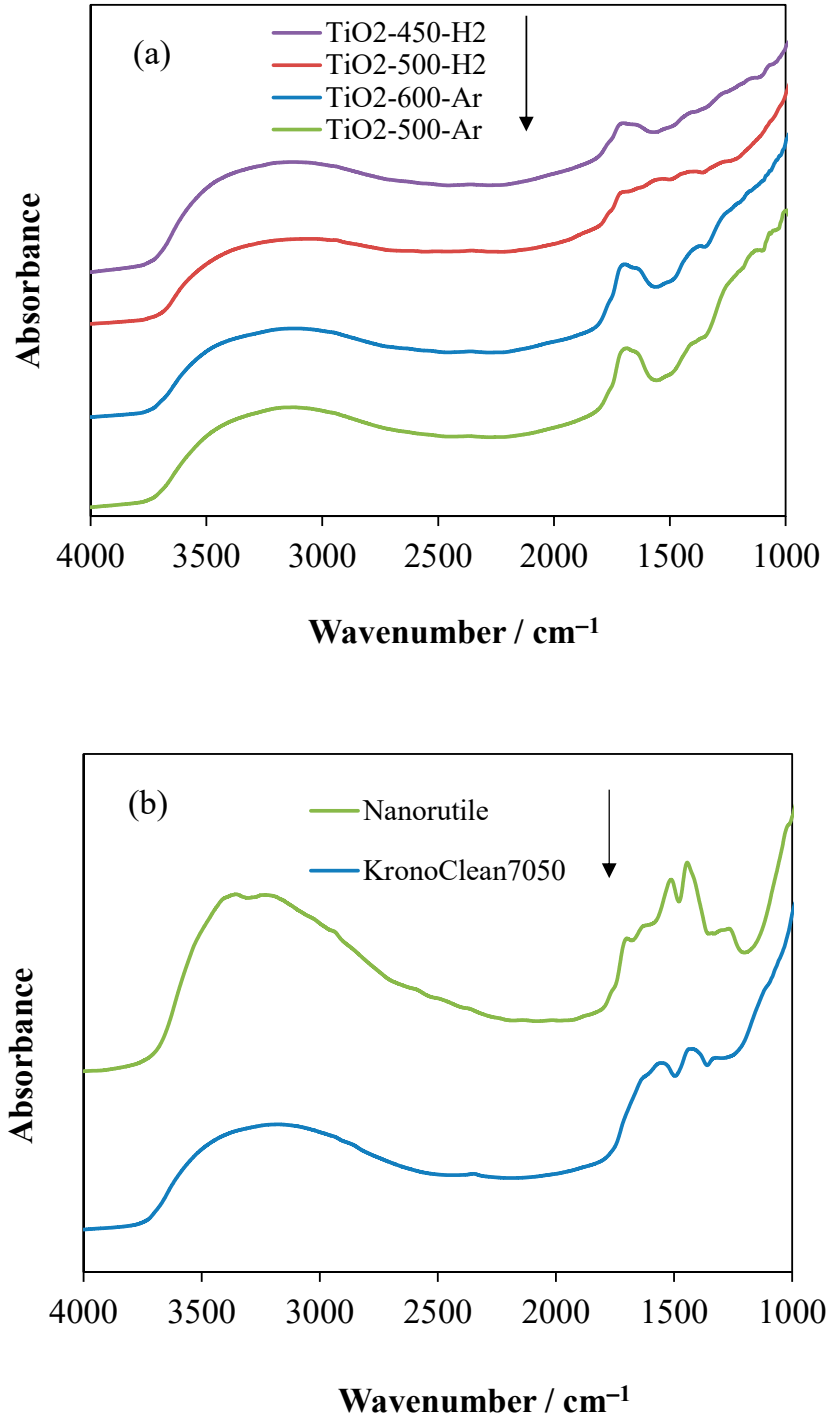

Figure 7. FTIR spectra of titania samples recorded after acetaldehyde adsorption: (**a**) prepared and (**b**) commercial.

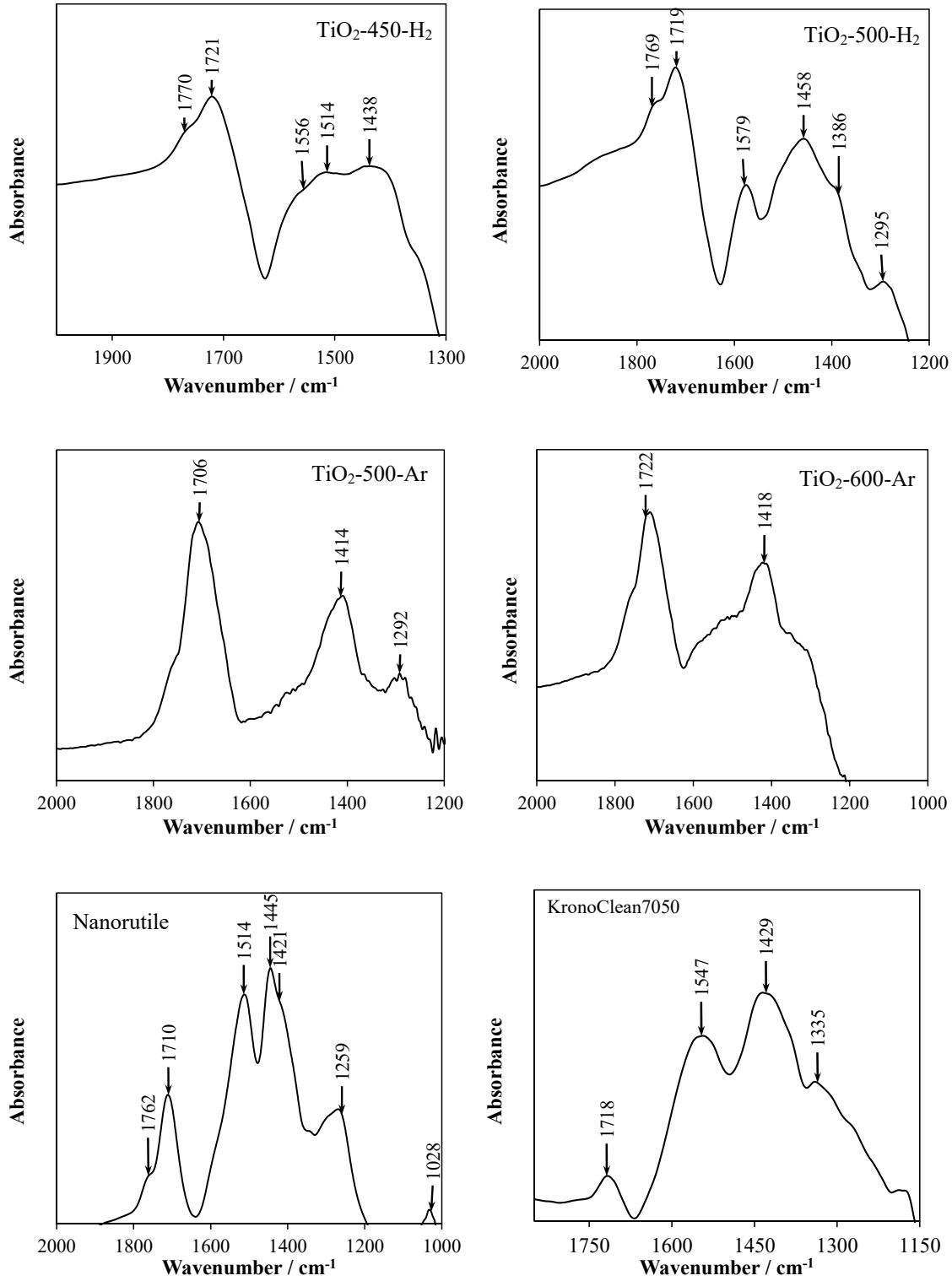

Figure 8. FTIR spectra of titania samples after acetaldehyde adsorption—subtracted from these before adsorption.

The bands at 1769 and 1719 cm^{-1} can be ascribed as ν(C=O) vibrations in the formate. Those at 1579 and 1295 cm^{-1} were $\nu_a(COO)_{aq}$ and ν(C–O) vibrations, respectively, and are characteristic to the presence of acetic acid. On the other hand, both bands at 1386 and 1458 cm^{-1} can be assigned to acetic acid $\delta(CH_3)$ and acetate ν(COO) [29]. FTIR spectrum of nanorutile showed high-intensity peaks at 1514, 1445, and 1259 cm^{-1}, which can be attributed to ν(COO) and CH_3 vibrations in the acetate and ν(C-C) in acetone,

respectively [1,29]. The band at 1421 cm^{-1} can be assigned to acetate $v_s(COO)_{ads}$. The band at 1710 cm^{-1} can be assigned to ν(C=O) vibration in acetone. An additional small intensity peak at 1762 cm^{-1} was observed, which can be assigned to ν(C=O) bound in formate. This means that partial oxidation of acetaldehyde to formate species on nanorutile could have occurred.

The commercial sample KRONOClean 7050 showed high-intensity bands at 1547 and 1429 cm^{-1}, assigned to ν(COO) vibrations in the acetate. An additional band at 1335 cm^{-1}, assigned to CH_3 group in acetate, confirmed that acetaldehyde was oxidized to acetate species on the surface of this sample. The band at 1718 cm^{-1} corresponded to C=O vibration in formate species [1].

In the next step, FTIR measurements were performed for titania samples after the photocatalytic process. The results are presented in Figure 9 for original and Figure 10 subtracted spectra.

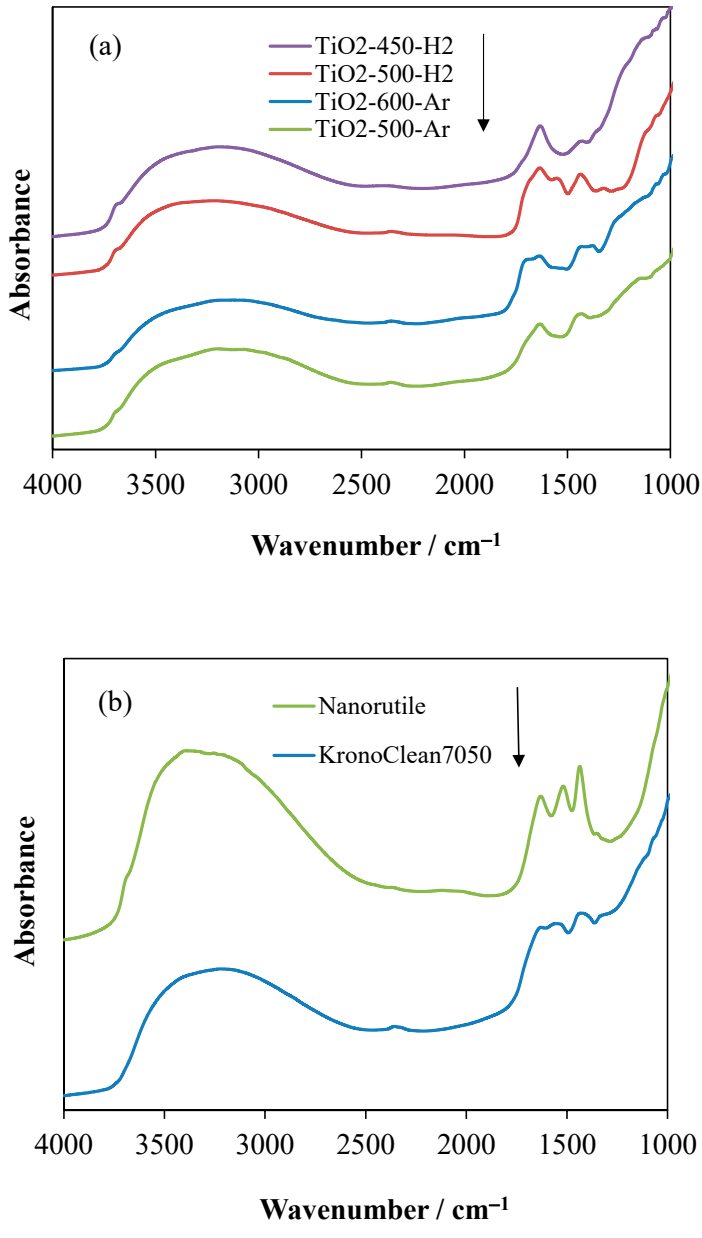

Figure 9. FTIR spectra of titania samples recorded after photocatalytic decomposition of acetaldehyde: (**a**) prepared and (**b**) commercial.

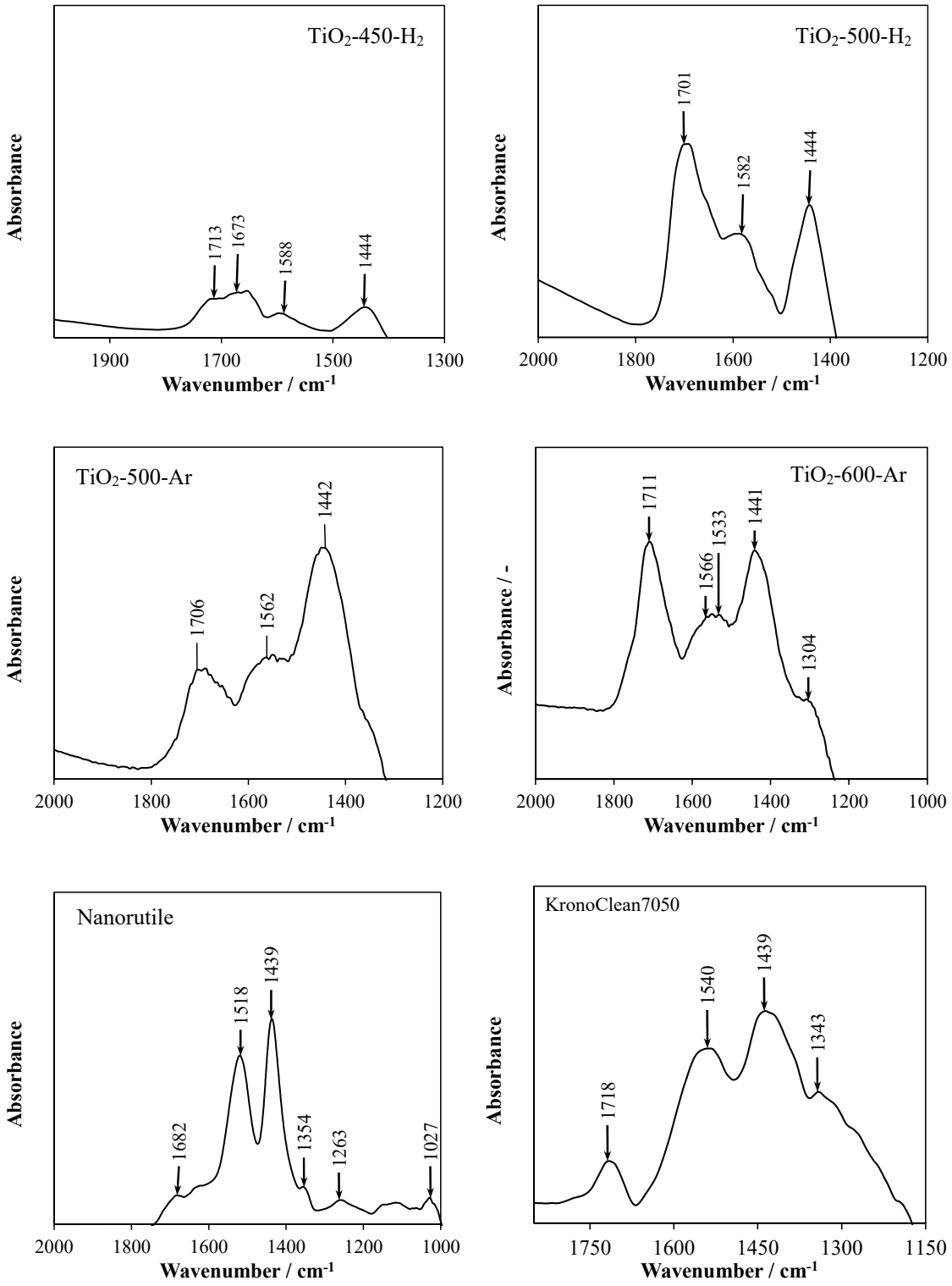

Figure 10. FTIR spectra of titania samples after photocatalytic decomposition of acetaldehyde—subtracted from these before adsorption.

In the case of nanorutile sample, the FTIR spectrum after photocatalysis was quite similar to that after acetaldehyde adsorption. Still, high intensity bands related to acetate species were observed (at 1514, 1445, and 1028 cm^{-1}). However, the peaks attributed to acetone (at 1710, 1421, and 1259 cm^{-1}) disappeared, and just a low-intensity peak at 1354 cm^{-1} assigned to ν(COO) vibrations in formate was observed. The, most probably, acetic acid

adsorbed on the rutile surface was not decomposed after photocatalytic process. A similar effect was observed by other researchers [29]. The anatase-type TiO_2 KRONOClean 7050 showed insignificant changes in FTIR spectrum after photocatalysis. The same bands were observed, just with lower intensity. A pronounced change in FTIR spectrum was noted for TiO_2-500-H_2 sample, and peaks assigned to formate species (at 1769 and 1719 cm^{-1}) disappeared, but acetate species (at 1582 and 1444 cm^{-1}) assigned to ν(COO) vibrations remained [1,29]. TiO_2 sample prepared in H_2 at 450 °C showed insignificant changes in FTIR spectrum after photocatalysis in comparison with the state before acetaldehyde adsorption. Low intensity peaks at 1713, 1588, and 1444 cm^{-1} assigned to ν(C=O), ν(COO), and $\nu(CH_3)$ vibrations in acetate were visible. Additionally, a small band at 1673 cm^{-1} assigned to ν(C=O) vibrations in acetic acid was observed. In the case of sample prepared at 500 °C in Ar, after photocatalysis a new band at 1562 cm^{-1} related to acetate species appeared and that which was characteristic to acetic acid ν(C-O) at 1292 cm^{-1} disappeared.

TPD measurements were performed in order to analyze formed products upon acetaldehyde adsorption on TiO_2 and its further photocatalytic transformation. The main product analyzed during thermal desorption was an acetic acid. However, for treated nanorutile and TiO_2-500-H_2 samples, acetone was also observed. High quantity of acetic acid desorption was noted for samples TiO_2-500-Ar and TiO_2-450-H_2 (Figure 11a). After the photocatalytic process, a part of the acetic acid was still present on the surface of the TiO_2-500-Ar sample, whereas on the latter sample (TiO_2-450-H_2) it was in trace amounts only, as shown in the TPD plot in Figure 11b. Titania sample heated at 600 °C in Ar did not show any pronounced desorption peaks during thermal heating up to 250 °C (Figure 11a,b). A certain similarity during analyses of thermal desorption peaks between nanorutile and TiO_2-500-H_2 samples was found. These samples did not expose any desorption peaks of an acetic acid, but instead of this, acetone species were identified (Figure 11c,d). The commercial anatase sample KRONOClean 7050 did not show any desorption peaks at this temperature program range.

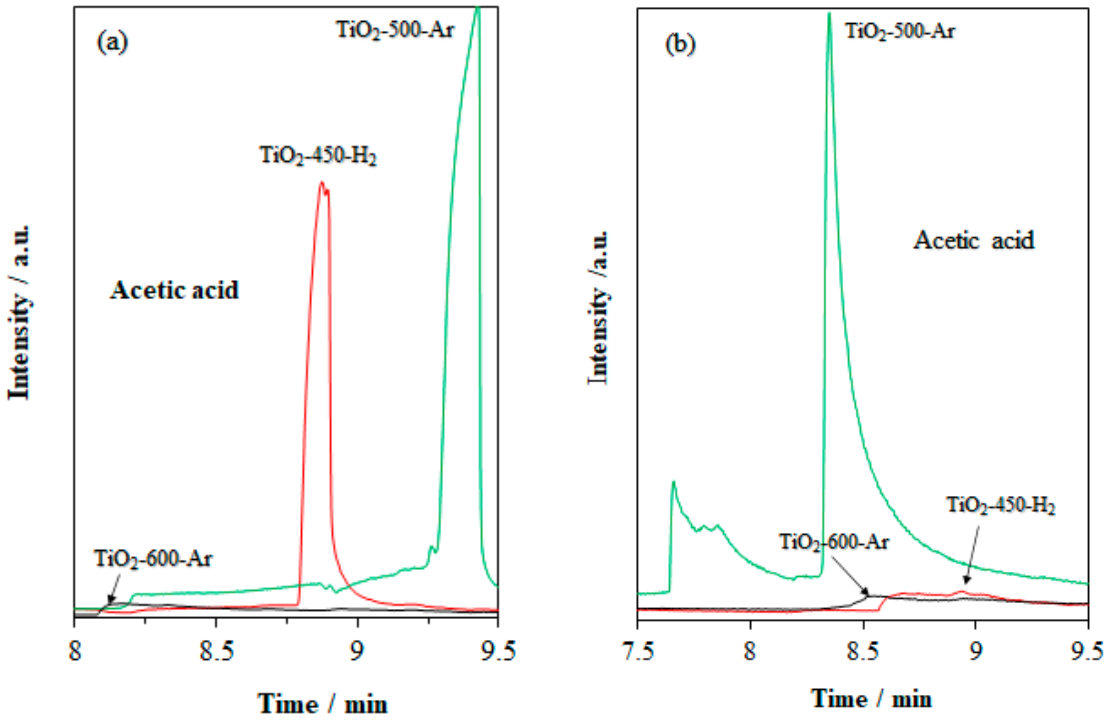

Figure 11. *Cont.*

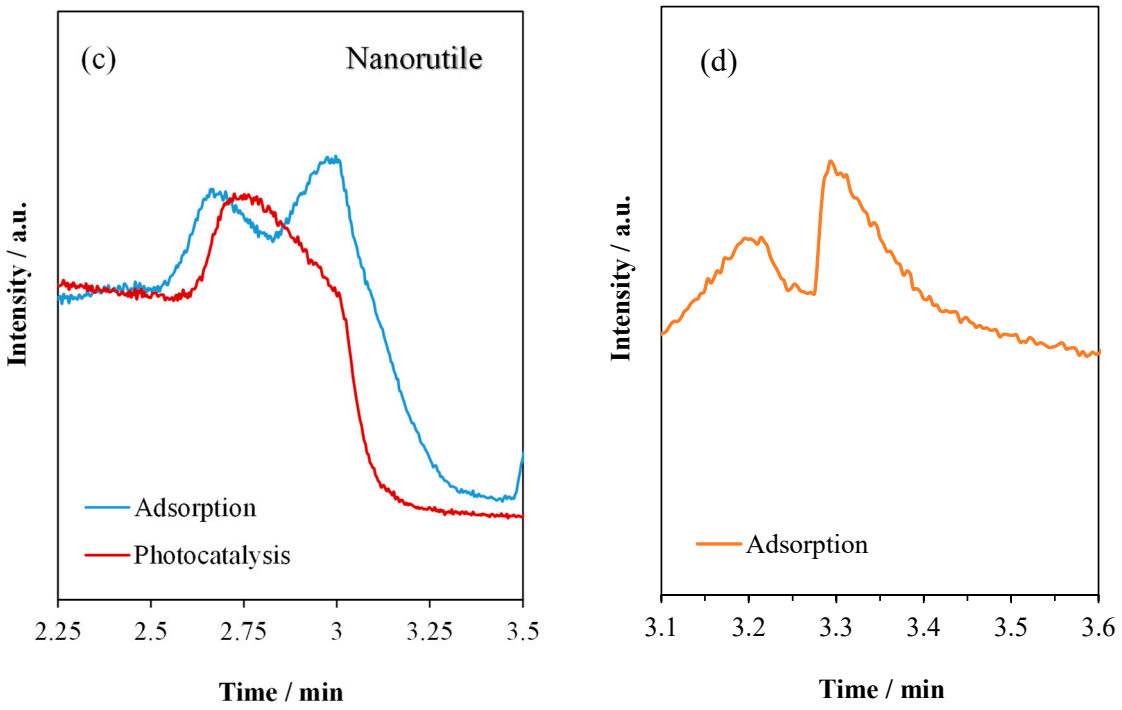

Figure 11. Thermal desorption peaks from titania samples heated up to 250 °C: (**a**) after adsorption of acetaldehyde, (**b**) after photocatalytic decomposition of acetaldehyde, (**c**) nanorutile, and (**d**) TiO_2-500-H_2.

3. Discussion

These results showed difference in the interaction of the titania surface with acetaldehyde between samples. Nanorutile and TiO_2 reduced under hydrogen treatment (TiO_2-500-H_2) revealed high adsorption of acetate species on FTIR spectra, the products of acetaldehyde decomposition. However, these species did not desorb during thermal treatment up to 250 °C and did not follow photocatalytic decomposition during illumination of a fluorescent lamp. These species were strongly bound to the titania surface. Similar observations were reported elsewhere for TiO_2 of rutile structure [13,29]. It was also reported that acetaldehyde formed butene complexes on rutile and reduced anatase through the coupling reaction of two paired acetaldehyde molecules adsorbed on the titania surface [13,14]. Moreover, it was reported that these complexes had high thermal stability and could impede acetaldehyde decomposition. According to the literature, the butene complexes desorb at the temperature of 530 K [13]. During performed TPD analyses, butene complexes were not detected, probably because of low temperature of programmed desorption. However, it is suspected that butene complexes were present on the nanorutile and TiO_2 reduced with H_2 at 500 °C, and acetone was a product of their decomposition.

Commercial titania KRONOClean 7050 showed some acetate and formate ionic species on the surface after interaction with acetaldehyde. However, these species were poorly analyzed during TPD analyses. It is most likely that they were binding with the anatase surface together with water molecules, because this sample had a highly hydroxylic surface. Moreover, this sample was highly porous and, most probably, desorption of these species could occur at higher temperatures. The titania sample prepared at 450 °C under hydrogen showed the highest rate of acetaldehyde decomposition among the other prepared samples. High interaction of acetaldehyde molecules with the surface of this sample resulted in high conversion to acetic acid in the dark and then rapid decomposition of all the adsorbed species during illumination of with a fluorescent lamp. Titania surface defects (hole traps) can increase adsorption and oxidation of acetaldehyde molecules. Formed upon oxidation, carbonyl radicals can take part in the chain reactions of acetaldehyde decomposition [5,8]. The group of Prof. A. Fujishima reported high conversion of acetaldehyde to acetic acid under weak UV irradiation of TiO_2 with high quantum yield, which was estimated to

be around 150%. Such high yield of acetic acid formation was a result of a radical-chain-type process [31]. This mechanism of acetaldehyde decomposition is beneficial, because occurring radical-chain reactions can conduce to efficient decomposition of acetaldehyde under indoor light.

Commercial titania KRONOClean 7050 also showed a high decomposition rate of acetaldehyde. However, after the photocatalytic process its surface was loaded with products of acetaldehyde decomposition, so this photocatalyst could be deactivated with the proceeding time of exploitation.

4. Materials and Methods

4.1. Preparation of Reduced TiO_2

Titania pulp was used as a source of TiO_2, which was received from the Chemical factory "Police" S.A. Grupa Azoty (Poland). This material was a semi-product obtained from titania white production and contained a few percent of sulfuric compounds. This product was taken after hydrolysis of titania but before the calcination process, so it had a mostly amorphous structure with a significant share of anatase crystallites, around 11%, and 3.5% of rutile nuclei, which are usually added before the calcination process to accelerate transformation of anatase into rutile. The measured surface area of a dried titania pulp was equal to 230 m^2/g and the average size of anatase crystallites determined from XRD measurements was equal to 7.6 nm. Preparation of the reduced TiO_2 consisted of two steps. In the first step, titania material underwent hydrothermal treatment at 150 °C in an autoclave for 1 h under pressure of 7.4 bars. In the next step, titania was dried at 100 °C overnight and then submitted to a heat-treatment process in a pipe furnace at temperatures of 400–500 °C under flow of hydrogen gas (30 mL/h). For comparison, heat-treatment of TiO_2 under Ar gas was performed.

4.2. Analytical Methods

The prepared samples were characterized by different analytical methods, such as: X-ray diffraction (XRD), UV-Vis and FTIR spectroscopies, EPR, nitrogen adsorption at 77 K, elemental analyses, zeta potential, and TPD (temperature-programmed desorption). The ability of photocatalysts for hydroxyl radical formation under UV-Vis light was measured in the aqueous solution by a fluorescence technique.

XRD measurements were performed in an Empyrean diffractometer from PANanalytical (Almelo, The Netherlands) with use of a Cu X-ray source, λ = 0.154439 nm. The measurements were performed in the 2θ range of 20–80° with step 0.05. The applied voltage was 35 KV and current 30 mA. The phase composition of TiO_2 was calculated from the equations:

$$X_R = \frac{I_R}{I_R + 0.75 I_A} \quad (1)$$

$$X_A = 1 - X_R \quad (2)$$

where:

X_A, X_R—molar fractions of anatase (A) and rutile (R),

I_A, I_R—intensities of reflexes of anatase (101) and rutile (110).

Coefficients used in Equation (1) were estimated on the bases of Reference Intensity Ratio (RIR) values for the identified phases of TiO_2 obtained from the database PDF4+.

The mean size of crystallites (D) was calculated from the Scherrer Equation (3):

$$d = \frac{K \cdot \lambda}{(\beta - b) \cdot \cos\theta} \quad (3)$$

where:

K—shape factor (K = 0.93),

λ—the wavelength of Cu lamp [nm],

β—the width of the peak at half the maximum intensity after subtraction of background [rad],

b—apparatus dilatation [rad],

θ—the diffraction angle [°].

UV-Vis/DRS spectroscopy was applied to investigate the impact of the introduced surface titania defects on the optical properties of titania samples. The measurements were performed in a V-650 spectrometer from Jasco (Tokyo, Japan). The spectra were recorded in the range of 200–800 nm with the scanning speed 1 nm/sec. As a reference, $BaSO_4$ was used. The obtained data were converted to the Kubelka–Munk function and then energies of the band gap were determined.

FTIR spectroscopy was performed for powdered titania samples as prepared, after adsorption of acetaldehyde and after the photocatalytic process. The measurements were performed in an FTIR 4200 spectrometer from Jasco by use of the reflection technique.

Spectra were recorded with a resolution of 4 cm^{-1} and a scanning speed of 1 nm/sec. The background was subtracted in each measurement spectrum.

Magnetic resonance experimentation was performed using a conventional X–band Bruker ELEXSYS E 500 CW–spectrometer operating at 9.5 GHz with 100 kHz magnetic fields modulation. The first derivative of the absorption spectra was recorded as a function of the applied magnetic field within a 0–1.4 T range. Temperature dependences of the spectra were recorded using the Oxford Instrument ESP, nitrogen-flow cryostat in a range of 77–300 K.

The sulfur content in TiO_2 was determined by EDXRFS (energy-dispersive X-ray fluorescence spectroscopy). For that purpose, the spectrometer Epsilon3 from PANanalytical was used, and the method of internal pattern was applied.

The BET surface area of samples was determined from the measurements of nitrogen adsorption at the temperature of 77 K in a QUADRASORB Si analyzer from Quantachrome (USA). Before adsorption, the samples were outgassing under vacuum at 150 °C for 12 h. For calculation of the specific surface area, BJH method was used.

The electrokinetic potential of titania samples was measured in a Zetasizer Nano ZS analyzer of Malvern Company. For measurements, the titania samples were dispersed in an aqueous solution and stirred by a magnetic stirrer.

Photoluminescence spectra were recorded in a fluorescence spectrometer Hitachi F-2500 using a low-temperature sample compartment accessory. The measurements were performed at the temperature of liquid nitrogen, at an excitation wavelength of 290 nm. The emission spectra were recorded in the range of 330–700 nm.

For TD (Thermal Desorption) experiments followed by GC-MS, the equipment used for the analysis was a gas chromatograph (Agilent Technologies 6890 N) in splitless mode with a cis4+(PTV) Gerstel injector and a horizontal Thermal Desorption System Gerstel TDS-2 coupled to a mass spectrometer (Agilent 5973 N) as a selective detector. An The Agilent 5973 N mass spectrometer based on an electron impact ionization (EI) source and a quadrupole analyzer. The equipment allows comparison of the problem spectrum with a collection of spectra stored in memory (Wiley 275 Mass Spectral Data Library, included with the MSD ChemStation software of the 6890 Agilent GC System).

The GC-MS system was fitted with the Agilent J&W Scientific DB-624 column (6% Cyanopropylphenyl/94% Dimethylpolysiloxane, inner diameter: 0.25 mm, length: 30 m, film: 1.4 mm, whose temperature working range is −20–260 °C).

An aliquot of sample was introduced in an empty TD Gerstel glass tube (Supelco, Bellefonte, PA USA). This tube was placed in the Thermal Desorption System at 40 °C, held for 0.5 min. The thermal desorption program consisted of a temperature ramp from 40 to 250 °C at a 60 °C/min rate, and the holding time at the maximum temperature was 6 min. The carrier gas was helium (100 mL/min) and the transfer line temperature was 300 °C. The desorbed compounds were cryofocused in the cooled injection (PTV injector cooled to −150 °C with liquid nitrogen) until the end of the desorption procedure. Then, the temperature was rapidly increased from −150 to 250 °C at a speed of 10 °C/s for 3 min,

transferring the compounds to the GC column by operating in solvent vent mode using a purge flow to split bent of 40 mL/min He for 2 min. The GC temperature program featured the following conditions: isothermal hold at 30 °C for 5 min, and; temperature ramp of 10 °C/min up to 250 °C, held for 5 min. The carrier gas was helium (1.4 mL/min). The MS system was operated in the solvent vent mode, under the following conditions: mass range, 30–350 u; ionization potential, 70 eV; source temperature, 230° C, and; MS quadrupole temperature, 150 °C.

4.3. Photocatalytic Tests

The activity of titania samples towards OH radical formation was measured through the photooxidation of the terephthalic acid in an aqueous solution. The formed reaction product was 2-hydroxyterephthalic acid, a highly fluorescent compound, which was analyzed in the fluorescence spectrometer. For illumination of titania, a UV-Vis solar lamp was used from Philips (The Netherlands). The emission spectrum of this lamp was measured using a USB4000 Fiber Optic Spectrometer (Ocean Optics). The results are illustrated in Figure 12.

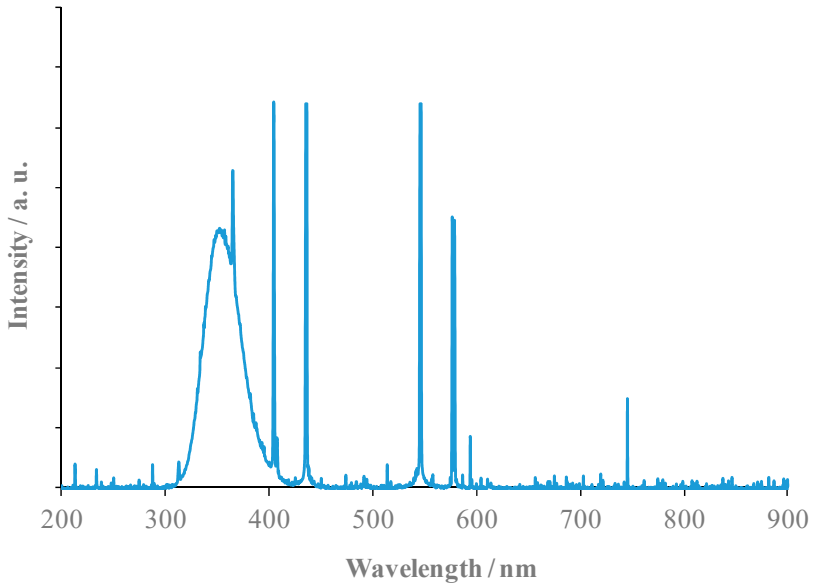

Figure 12. The emission spectrum of the UV-Vis solar lamp (Philips).

The photocatalytic tests were performed for the synthesized samples and two commercial ones, "nanorutile" produced by Sachtleben (Krefeld, Germany) and nanocrystalline anatase KRONOClean 7050, produced by Kronos International Ltd. (Germany).

Photocatalytic decomposition of gaseous acetaldehyde was carried out in the photocatalytic quartz reactor, which was irradiated by the fluorescence lamps. The emission spectrum of this lamp was also measured using a USB4000 Fiber Optic Spectrometer. See Figure 13.

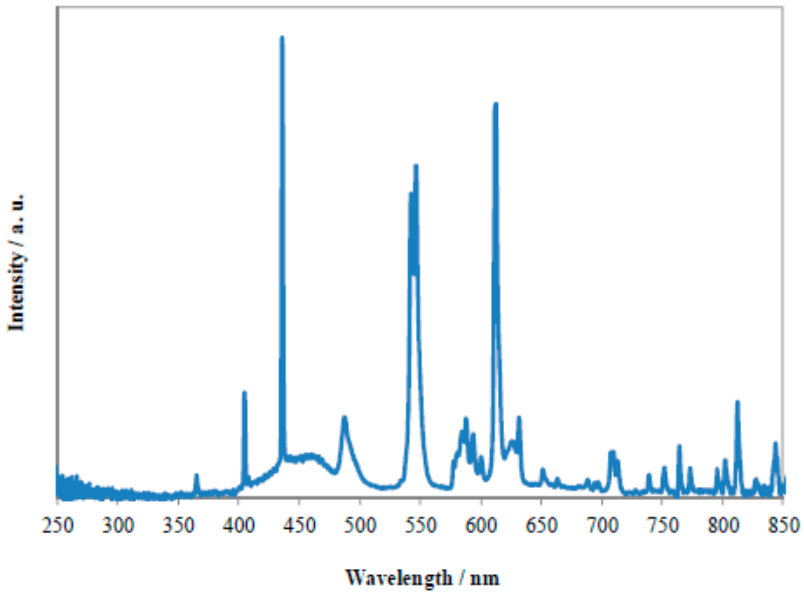

Figure 13. The emission spectrum of a fluorescent lamp.

Additionally, two sensors were applied (CM3 Kipp & Zonen Pyranometer and PD204AB Cos Macam Photometrics Ltd., The Netherlands) to measure the radiation intensity in the range of UV-Vis-NIR and UV-AB. These intensities were equal to 72.6 and 0.7 W/m^2 for UV-Vis-NIR and UV-AB ranges, respectively.

This photoreactor was mounted inside the thermostatic chamber. The process was conducted at a temperature of 25 °C, and gaseous model pollutant was supplied to the reactor from the bottle, which contained mixture of dry synthetic air and acetaldehyde (300 ppm). The photocatalytic samples were coated on the glass plates with dimension 20 mm × 20 mm, then six plates were placed inside the reactor, so the total reactive surface was equal to 24 cm^2. At first, the gas was flowing through the reactor and acetaldehyde was adsorbed on the titania surface. After stabilization of acetaldehyde concentration in the space chamber, the lamps were switched on and then the photocatalytic process began. The concentration of the acetaldehyde was measured in a gas chromatograph with an FID detector. At the same time, concentration of CO_2 was measured in the outlet stream by CO_2 sensor. The scheme of the photocatalytic installation system was reported elsewhere [17].

5. Conclusions

This study showed high impact of $O^{\bullet -}$ titania surface defects on the photocatalytic oxidation of acetaldehyde. Formed hole traps upon hydrogenation of TiO_2 at 450 °C could increase oxidation of acetaldehyde, which was adsorbed on the titania surface. The quantum yield of this reaction was over 100%, because of the chain-reaction mechanism involved. Such defected structure can increase the amount of terminal OH groups, which take part in the hydroxyl radical formation. These radicals can significantly improve the mineralization process of the acetic acid. Hydrogenation of TiO_2 at 500 °C conduced to formation of Ti^{3+} defects and oxygen vacancies. Formed titania surface defects in these conditions improved separation of free carriers. However, acetaldehyde molecules were adsorbed at different active sites than in the case of sample prepared at 450 °C under hydrogen. The most probably in TiO_2 containing Ti^{3+} and oxygen vacancy, acetaldehyde was adsorbed at the oxygen vacancy sites via aldehyde group and then from two adsorbed acetaldehyde molecules, some oxygen-butene complexes were formed on titania surface, which were followed oxidation to the acetic acid. Formed in this way, acetic acid was strongly bound with the titania surface and did not follow vulnerable photocatalytic decomposition. In fact, such defected titania structure impedes the total mineralization of adsorbed acetaldehyde molecules. Prepared TiO_2 under hydrogen treatment at 500 °C

showed a similar mechanism of acetaldehyde decomposition as nanorutile, which has lower oxidation properties than anatase. This means that formation of oxygen vacancies and electron traps in TiO_2 increase its reductive properties, which change the mechanism of acetaldehyde decomposition. This study showed the high impact of carbonyl radicals on acetaldehyde decomposition. These carbonyl radicals were formed upon oxidation with hole traps. Such a mechanism of acetaldehyde decomposition was earlier reported by the group of Prof. A. Fujishima [5,8,31]. This study showed that this mechanism is the most favorable in rapid decomposition of acetaldehyde. The properties of titania towards acetaldehyde decomposition can be improved via hydrogenation process at a low temperature such as 450 °C, but at a higher temperature of TiO_2 treatment Ti^{3+} centers are formed, that make the mechanism of acetaldehyde decomposition less efficient.

Supplementary Materials: The following are available online at https://www.mdpi.com/article/10.3390/catal11111281/s1, Figure S1: UV-Vis/DR spectra of TiO_2 samples heat-treated under (**a**) hydrogen, and (**b**) argon.

Author Contributions: Conceptualization, B.T.; methodology, B.T., H.F., M.Á.L.-R., M.C.R.-M.; formal analysis, P.R., H.F., M.Á.L.-R.; data curation, P.R., B.T., H.F., M.Á.L.-R., M.C.R.-M.; writing—original draft preparation, P.R.; writing—review and editing, B.T.; visualization, P.R., B.T., H.F., M.Á.L.-R., M.C.R.-M.; supervision, B.T.; project administration, B.T.; funding acquisition, B.T. All authors have read and agreed to the published version of the manuscript.

Funding: This research was funded by the National Science Centre, Poland, grant nr 2020/39/B/ST8/01514.

Data Availability Statement: There are new data, not published elsewhere.

Conflicts of Interest: The authors declare no conflict of interest.

References

1. Tryba, B.; Rychtowski, P.; Markowska-Szczupak, A.; Przepiórski, J. Photocatalytic Decomposition of Acetaldehyde on Different TiO_2-Based Materials: A Review. *Catalysts* **2020**, *10*, 1464. [CrossRef]
2. Shah, K.W.; Li, W. A Review on Catalytic Nanomaterials for Volatile Organic Compounds VOC Removal and Their Applications for Healthy Buildings. *Nanomaterials* **2019**, *9*, 910. [CrossRef]
3. Shayegan, Z.; Lee, C.-S.; Haghighat, F. TiO2 photocatalyst for removal of volatile organic compounds in gas phase—A review. *Chem. Eng. J.* **2018**, *334*, 2408–2439. [CrossRef]
4. Nag, P.K. Sick Building Syndrome and Other Building-Related Illnesses. In *Office Buildings*; Design Science and Innovation; Springer: Singapore, 2019; pp. 53–103. ISBN 9789811325762.
5. Fujishima, A.; Rao, T.N.; Tryk, D.A. Titanium Dioxide Photocatalysis. *J. Photochem. Photobiol. C Photochem. Rev.* **2000**, *1*, 1–21. [CrossRef]
6. Fujishima, A.; Zhang, X.; Tryk, D. Heterogeneous photocatalysis: From water photolysis to applications in environmental cleanup. *Int. J. Hydrogen Energy* **2007**, *32*, 2664–2672. [CrossRef]
7. Nakata, K.; Fujishima, A. TiO_2 photocatalysis: Design and applications. *J. Photochem. Photobiol. C Photochem. Rev.* **2012**, *13*, 169–189. [CrossRef]
8. Pitchaimuthu, S.; Honda, K.; Suzuki, S.; Naito, A.; Suzuki, N.; Katsumata, K.; Nakata, K.; Ishida, N.; Kitamura, N.; Idemoto, Y.; et al. Solution Plasma Process-Derived Defect-Induced Heterophase Anatase/Brookite TiO_2 Nanocrystals for Enhanced Gaseous Photocatalytic Performance. *ACS Omega* **2018**, *3*, 898–905. [CrossRef] [PubMed]
9. Di Valentin, C.; Fittipaldi, D. Hole Scavenging by Organic Adsorbates on the TiO_2 Surface: A DFT Model Study. *J. Phys. Chem. Lett.* **2013**, *4*, 1901–1906. [CrossRef] [PubMed]
10. Tryba, B.; Rychtowski, P.; Srenscek-Nazzal, J.; Przepiorski, J. The Inflence of TiO_2 Structure on the Complete Decomposition of Acetaldehyde Gas. *Mater. Res. Bull.* **2020**, *126*, 110816. [CrossRef]
11. Batault, F.; Thevenet, F.; Hequet, V.; Rillard, C.; Le Coq, L.; Locoge, N. Acetaldehyde and Acetic Acid Adsorption on TiO_2 under Dry and Humid Conditions. *Chem. Eng. J.* **2015**, *264*, 197–210. [CrossRef]
12. Mahmood, A.; Shi, G.; Xie, X.; Sun, J. Assessing the Adsorption and Photocatalytic Activity of TiO_2 Nanoparticles for the Gas Phase Acetaldehyde: A Computational and Experimental Study. *J. Alloys Compd.* **2020**, *819*, 153055. [CrossRef]
13. Plata, J.J.; Collico, V.; Márquez, A.M.; Sanz, J.F. Understanding Acetaldehyde Thermal Chemistry on the TiO_2 (110) Rutile Surface: From Adsorption to Reactivity. *J. Phys. Chem. C* **2011**, *115*, 2819–2825. [CrossRef]
14. Ji, Y.; Zheng, Y.; Ma, X.; Cui, X.; Wang, B. Role of Reduced Defects for Coupling Reactions of Acetaldehyde on Anatase TiO_2 (001)-(1 × 4) Surface. *Chin. J. Chem. Phys.* **2019**, *32*, 417–422. [CrossRef]

15. Hauchecorne, B.; Terrens, D.; Verbruggen, S.; Martens, J.A.; Van Langenhove, H.; Demeestere, K.; Lenaerts, S. Elucidating the Photocatalytic Degradation Pathway of Acetaldehyde: An FTIR in Situ Study under Atmospheric Conditions. *Appl. Catal. B Environ.* **2011**, *106*, 630–638. [CrossRef]
16. Melchers, S.; Schneider, J.; Emeline, A.; Bahnemann, D. Effect of H_2O and O_2 on the Adsorption and Degradation of Acetaldehyde on Anatase Surfaces-An In Situ ATR-FTIR Study. *Catalysts* **2018**, *8*, 417. [CrossRef]
17. Tryba, B.; Wozniak, M.; Zolnierkiewicz, G.; Guskos, N.; Morawski, A.; Colbeau-Justin, C.; Wrobel, R.; Nitta, A.; Ohtani, B. Influence of an Electronic Structure of N-TiO_2 on Its Photocatalytic Activity towards Decomposition of Acetaldehyde under UV and Fluorescent Lamps Irradiation. *Catalysts* **2018**, *8*, 85. [CrossRef]
18. Hu, Y.; Xie, X.; Wang, X.; Wang, Y.; Zeng, Y.; Pui, D.Y.H.; Sun, J. Visible-Light Upconversion Carbon Quantum Dots Decorated TiO_2 for the Photodegradation of Flowing Gaseous Acetaldehyde. *Appl. Surf. Sci.* **2018**, *440*, 266–274. [CrossRef]
19. Carrera, R.; Vázquez, A.L.; Castillo, S.; Arce Estrada, E.M. Photocatalytic Degradation of Acetaldehyde by Sol-Gel TiO_2 Nanoparticles: Effect of the Physicochemical Properties on the Photocatalytic Activity. *MSF* **2011**, *691*, 92–98. [CrossRef]
20. Tryba, B.; Jafari, S.; Sillanpää, M.; Nitta, A.; Ohtani, B.; Morawski, A.W. Influence of TiO_2 Structure on Its Photocatalytic Activity towards Acetaldehyde Decomposition. *Appl. Surf. Sci.* **2019**, *470*, 376–385. [CrossRef]
21. Di Valentin, C.; Pacchioni, G.; Selloni, A. Reduced and N-Type Doped TiO_2: Nature of Ti^{3+} Species. *J. Phys. Chem. C* **2009**, *113*, 20543–20552. [CrossRef]
22. Naldoni, A.; Altomare, M.; Zoppellaro, G.; Liu, N.; Kment, Š.; Zbořil, R.; Schmuki, P. Photocatalysis with Reduced TiO_2: From Black TiO_2 to Cocatalyst-Free Hydrogen Production. *ACS Catal.* **2019**, *9*, 345–364. [CrossRef]
23. Chen, S.; Wang, Y.; Li, J.; Hu, Z.; Zhao, H.; Xie, W.; Wei, Z. Synthesis of Black TiO_2 with Efficient Visible-Light Photocatalytic Activity by Ultraviolet Light Irradiation and Low Temperature Annealing. *Mater. Res. Bull.* **2018**, *98*, 280–287. [CrossRef]
24. Ullattil, S.G.; Narendranath, S.B.; Pillai, S.C.; Periyat, P. Black TiO_2 Nanomaterials: A Review of Recent Advances. *Chem. Eng. J.* **2018**, *343*, 708–736. [CrossRef]
25. Kumar, C.P.; Gopal, N.O.; Wang, T.C.; Wong, M.-S.; Ke, S.C. EPR Investigation of TiO_2 Nanoparticles with Temperature-Dependent Properties. *J. Phys. Chem. B* **2006**, *110*, 5223–5229. [CrossRef] [PubMed]
26. Colbeau-Justin, C. Structural influence on charge-carrier lifetimes in TiO_2 powders studied by microwave absorption. *J. Mater. Sci.* **2003**, *38*, 2429–2437. [CrossRef]
27. Buchalska, M.; Kobielusz, M.; Matuszek, A.; Pacia, M.; Wojtyła, S.; Macyk, W. On Oxygen Activation at Rutile- and Anatase-TiO_2. *ACS Catal.* **2015**, *5*, 7424–7431. [CrossRef]
28. Tryba, B.; Tygielska, M.; Orlikowski, J.; Przepiórski, J. Influence of TiO_2 Hydrophilicity on the Photocatalytic Decomposition of Gaseous Acetaldehyde in a Circulated Flow Reactor. *Reac. Kinet. Mech. Cat.* **2016**, *119*, 349–365. [CrossRef]
29. Mattsson, A.; Österlund, L. Adsorption and Photoinduced Decomposition of Acetone and Acetic Acid on Anatase, Brookite, and Rutile TiO_2 Nanoparticles. *J. Phys. Chem. C* **2010**, *114*, 14121–14132. [CrossRef]
30. Tryba, B.; Tygielska, M.; Colbeau-Justin, C.; Kusiak-Nejman, E.; Kapica-Kozar, J.; Wróbel, R.; Żołnierkiewicz, G.; Guskos, N. Influence of PH of Sol-Gel Solution on Phase Composition and Photocatalytic Activity of TiO_2 under UV and Visible Light. *Mater. Res. Bull.* **2016**, *84*, 152–161. [CrossRef]
31. Ohko, Y.; Tryk, D.A.; Hashimoto, K.; Fujishima, A. Autoxidation of Acetaldehyde Initiated by TiO_2 Photocatalysis under Weak UV Illumination. *J. Phys. Chem. B* **1998**, *102*, 2699–2704. [CrossRef]